Bluetooth Low Energy-based Angle of Arrival Estimation via Switch Antenna Array for Indoor Localization

Conference Paper · July 2020

DOI: 10.23919/FUSION45008.2020.9190573

CITATIONS
65

READS
5,952

4 authors, including:

Zohreh H. Meybodi
Concordia University
37 PUBLICATIONS **439** CITATIONS

SEE PROFILE

Konstantinos Plataniotis
University of Toronto
831 PUBLICATIONS **26,283** CITATIONS

SEE PROFILE

Arash Mohammadi
Concordia University
289 PUBLICATIONS **6,594** CITATIONS

SEE PROFILE

Bluetooth Low Energy-based Angle of Arrival Estimation via Switch Antenna Array for Indoor Localization

1sh Zohreh Hajiakhondi-Meybodi
Electrical & Computer Engineering,
Concordia University,
Montreal, Canada
z_hajiak@encs.concordia.ca

2nd Mohammad Salimibeni
Concordia Institute for Inf. Systems Eng.,
Concordia University,
Montreal, Canada
m_alimib@encs.concordia.ca

3th Konstantinos N. Plataniotis
Electrical & Computer Engineering,
University of Toronto,
Toronto, Canada
kostas@ece.utoronto.ca

4th Arash Mohammadi
Concordia Institute for Inf. Systems Eng.,
Concordia University,
Montreal, Canada
arash.mohammadi@concordia.ca

***Abstract*—With expected widespread implementation of 5G networks and 5G Internet of Things (IoT), indoor localization is expected to become of even further importance. Although Global Positioning System (GPS) ensures efficient outdoor localization, generally speaking, indoor localization systems fail to provide the same level of efficiency. In this regard, there has been recent widespread attention to Angle of Arrival (AoA) with the application on Switch Antenna Array (SAA), as an efficient indoor localization method due to its potential in determining location with low estimation error. The AoA, however, suffers from several issues including being sensitive to multipath effects, noise, fluctuations of received signal, and frequency/phase shifts. To tackle these issues, the paper proposes a set of signal processing and information fusion methods by integration of Nonlinear Least Square (NLS) curve fitting, Kalman Filter (KF), and Gaussian Filter (GF) to boost the accuracy rate of estimated angle. The proposed fusion framework is evaluated based on a real Bluetooth Low Energy (BLE) dataset and results illustrate significant potentials in terms of improving overall BLE-based achievable accuracy in angle detection.**

***Index Terms*—Internet of Things, Indoor Localization, Switch Antenna Array, Bluetooth Low Energy, Angle of Arrival Estimation.**

I. Introduction

Recent developments and advancements in the Internet of Things (IoT), low power wireless networks, and processing methodologies have resulted in the emergence of several different and innovative indoor localization technologies, including Infrared (IR) systems [1], Ultrasonic (US) systems [2], and Optical-based frameworks [3]. These systems share several common underlying properties, such as being sensitive to multipath effects, high costs and complexity and in some cases, and not being readily available [4]. Consequently, the main focus of researchers has been shifted to Radio Frequency (RF) indoor localization technologies, including Radio-Frequency IDentification (RFID) [5], ZigBee [6], WiFi [7], Bluetooth Low Energy (BLE) [8], and Ultra Wide Band (UWB) [9]. There are several notable factors that should be considered in developing an indoor localization system, such as cost, accuracy, robustness, scalability, power requirements, reliability, and coverage. Over the last few decades, there has been a significant surge of interest for BLE-based technologies, as one of the most reliable RF-based localization frameworks due to its availability (e.g., BLE is available on most modern smart devices), low power consumption, and low cost [10].

Literature Review: BLE is a commonly used low-power wireless protocol for IoT applications. Bluetooth beacons are small radio transmitters that send signals within upto 100 m radius. Bluetooth beacons, supported by many systems, are cost effective and are able to accurately determine the location of user devices upto few meters. There are numerous indoor location schemes that works on different aspects of BLE received signal. For instance, Received Signal Strength (RSS)-based methods [11] determine the location of user devices based on the strength of the signal, received by BLE beacons, while Angle of Arrival (AoA) [12] and Time of Arrival (ToA) [13] schemes evaluate the angle and the time of the incident signal, respectively. AoA localization is a nonlinear estimation problem to determine the source position based on the propagation direction of an incident radio frequency wave from an antenna array, such as Switch Antenna Array (SAA), which has been an active research field for several decades. One of the early research efforts in AoA framework for BLE technology exploited the MUltiple Signal CLassification (MUSIC) algorithm [12]. The authors in [14] introduced a closed-form algebraic solution for AoA localization with Bayesian

This work was partially supported by the Natural Sciences and Engineering Research Council (NSERC) of Canada through the NSERC Discovery Grant RGPIN-2016-04988.

priors, which is capable of providing highly accurate source position estimates with low computational complexity. Such an approach, however, suffers from severe bias problems.

Reference [15] determined the angle of incident signal based on the phase difference between the In-phase/Quadrature (I/Q) samples received by an antenna array. This paper investigated effects of the unbalanced carrier frequency of the transmitter and receiver. The authors in [16] investigated performance of AoA localization capability, incorporated in the recently introduced BLE 5.1 standard, to illustrate impact of different channels of BLEs on the accuracy rate of angle detection. One of the most crucial limitation of conventional AoA estimation methods is that they do not take into account the effect of switching antenna on I/Q samples. In addition, different BLE channels experience different interference with WiFi, leading to modest positioning accuracy when relying on phase difference. To tackle these problems, this paper is concerned with design of processing and information fusion solutions to reconstruct reliable signals from raw I/Q samples.

Contribution In this paper, we leverage the phase difference of I/Q samples obtained from SAA to achieve a fine-grained localization. Compared to the RSS, that attenuates quickly over the signal transmission in a fixed position, the phase difference can be estimated much more accurately as long as the signal-to-noise ratio is not too small. Despite all the benefits that comes with BLE-based AoA localization, there are, however, several associated drawbacks. More specifically, I/Q samples are sensitive to multipath effects, noise, fluctuations of received signal, and frequency and phase shiftings. In this paper, the motivation is to put one step forward to yield a higher accuracy in location estimation scheme based on the angle of incident signal received by BLE beacons. To be practical and in order to analyze raw data, it is vital to compensate the aforementioned negative effects by employing efficient processing and fusion techniques prior to utilization. The paper focuses on implementation of a processing framework concerned with analyzing the raw data with the aim of achieving potentially better representations of wireless data. The proposed processing consists of the following three phases:

- *Nonlinear Least Square (NLS) curve fitting*, which is applied on raw I/Q samples to eliminate the noise effect.
- *Kalman Filter (KF) Smoothing*: As a consequence of the frequency and phase shiftings and switching between elements in SAA, the phase difference obtained from different samples are not similar. To overcome this problem, we employ a Kalman Filter (KF) on the phase differences obtained from raw I/Q samples.
- *Gaussian Filter (GF)*, which is introduced to compensate the impact of different BLE channels on the accurate angle estimation.

To evaluate the effectiveness of our proposed processing framework, we set up a pilot study system that consists of a Real-Time Location System (RTLS) master, RTLS slave, and RTLS Passive including two array antennas each with three elements.

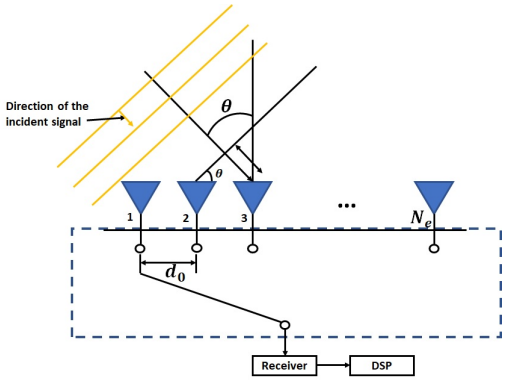

Fig. 1. Block diagram of SAA system model and AoA calculation.

The rest of the paper is organized as follows: In Section II, the wireless signal model is described and the main assumptions required for implementation of the proposed framework are introduced. Section III represents the proposed signal processing/fusion methods applying on phase differences. Section IV presents experimental results. Finally, Section V concludes the paper.

II. Wireless Signal Model

A. Switch Antenna Array

In AoA-based techniques, raw data including I/Q samples are provided as the input of an AoA-based localization approach. An I/Q sample includes the amplitude and the angle of the wave, defined as a set of Cartesian coordinates, that can be transformed into Polar coordinates to obtain the angle and the amplitude of the signal. To calculate the incident direction of radio waves, it is essential to measure the phase of an incoming signal by two or more antennas. As shown in Fig. 1, SAA is a combination of N_e number of connected antennas, named elements, and one receiver that switches to the receiving element in each time slot. Each element of the SAA receives the continuous-time signal $r(t)$, which is sampled by Analog to Digital (A/D) converter at a rate of $f_s = 1/T_s$ samples per second. Therefore, a discrete version of the received signal denoted by $\mathbf{r}_n$ is generated as

$$\mathbf{r}_n \triangleq \mathbf{r}[n] = \mathbf{r}_I[n] + j\mathbf{r}_Q[n]. \tag{1}$$

It is assumed that each transmitted packet consists of N_p samples, where each element collects N samples in each snapshot for a period of T, then it switches to the next element. In the other words, each packet consists of M snapshots, where $M = N_p/N$, and each element collects $m = M/N_e$ snapshots during one packet. To analyze I/Q samples, raw complex data vector $\mathbf{r}_n$ is transformed into $(mN) \times N_e$ matrix

$$\mathbf{R} = \begin{bmatrix} r_{1,1} & \cdots & r_{1,N_e} \\ \vdots & \vdots & \vdots \\ r_{N,1} & \cdots & r_{N,N_e} \\ \vdots & \vdots & \vdots \\ r_{mN,1} & \cdots & r_{mN,N_e} \end{bmatrix}, \tag{2}$$

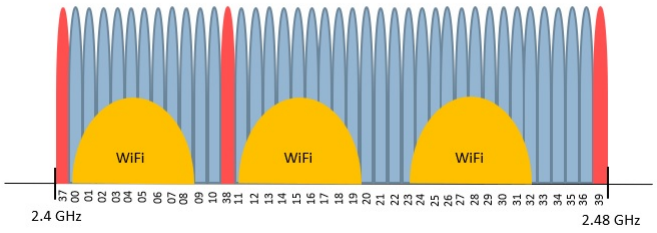

Fig. 2. The 2.4 GHz frequency band shared by BLE and WiFi. Red channels are the advertisement and the blue ones are data channels used by BLE.

where the k^{th} column of $\mathbf{R}$, indicates samples gathered by element e_k, for $(1 \leq k \leq N_e)$, during one packet. Consequently, matrix $\mathbf{R}$ is mapped into the phase $\mathbf{R}_\phi$ and magnitude $\mathbf{R}_A$ matrices, where $r_{\phi_{l,k}}$ and $r_{A_{l,k}}$ are obtained as follows:

$$r_{\phi_{l,k}} = \arctan\left(\frac{r_{Q_{l,k}}}{r_{I_{l,k}}}\right), \quad (3)$$

$$r_{A_{l,k}} = (r^2_{I_{l,k}} + r^2_{Q_{l,k}})^{\frac{1}{2}}, \quad (4)$$

To calculate the phase difference between two I/Q samples collected by two distinct elements, samples gathered from μ^{th} snapshot, for $(1 \leq \mu \leq m)$, from element e_i, denoted by $\mathbf{x}_i = [x_{(1+(1-\mu)N),i}, \ldots, x_{\mu N,i})]^T$, where $x_{l,i} = r_{A_{l,i}} e^{j r_{\phi_{l,i}}}$ is multiplied by the complex conjugate of samples from element e_j in the same snapshot, denoted by $\mathbf{x}_j$, as follows

$$\mathbf{\Delta\Phi}^{(i,j)} = \mathbf{x}_i \times \mathbf{x}_j^*, \quad (5)$$

where $\Delta\Phi^{(i,j)}_{l,1} = r_{A_{l,i}} r_{A_{l,j}} e^{j(r_{\phi_{l,i}} - r_{\phi_{l,j}})}$. Then, with a known spacing between the adjacent element, denoted by d_0, the angle of incident signal can be calculated as follows [17]

$$\boldsymbol{\theta}^{(i,j)} = \arcsin \frac{\lambda \mathbf{\Delta\Phi}^{(i,j)}}{2\pi d_{i,j}}, \quad (6)$$

where $\lambda = c/f$ and f denote the wave length and the carrier frequency of the signal, respectively. Moreover, c is the speed of light, about $3 \times 10^8 m/s$, and $d_{i,j} = |j - i| d_0$. Finally, $\theta_{estimate}$ is determined as the mean of a set of $\boldsymbol{\theta}^{(i,j)}$.

B. Wireless Communication Using BLE

One of the noticeable challenges of wireless technologies for IoT applications is high power consumption. BLE as one of the prominent Wireless Personal Area Network (WPAN) standards has paved the way for emergence of IoT applications. BLE employs Gaussian Frequency Shift Keynig (GFSK) modulation, with the transmission power of -20 to $+20$ dBm. It operates in 2.4 to 2.48 GHz frequency range, which is the same spectrum as WiFi. It is designed to operate at a distance of 10 to 100 m, though typically at 10 m or less. It uses 40 channels, including 37 data channels and 3 advertisement channels with 2 MHz bandwidth. From the channel perspective, as it can be seen in Fig. 2, the spectrum of WiFi and BLE overlap with each other in several channels. Therefore, to obtain an accurate angle, it is essential to consider the interference of WiFi on BLE. By considering the distribution of interference and noise in different BLE channels, we can find the most reliable angles. Moreover, BLE's operation mode come with Frequency Hopping (FH) method, allowing the modules to jump on data channels to avoid interference within BLE channels.

There are two different modes for data transmission on BLEs, including broadcast mode and connected mode. Devices use the broadcast mode to advertise their presence, including some information about the device type, manufacturer, operating on advertisement channels. Once one of the advertised beacons has been received on the broadcast bands, another device (master) initiates a connection to this device (slave). The master and the slave devices agree on several connection parameters during the connection establishment process, one of which is the frequency hop distance, denoted by f_{hop}. In order to send each packet, master and slave devices hop through the 37 data channels by f_{hop} bands. Because the total number of channels is prime 37, the transmissions jump through all accessible bands before repeating a channel that was previously used [18].

III. Wireless Signal Processing/Fusion Framework

Our system model consists of user devices that are required to be found (localized), and known location BLEs embedded with SAA. Once a user device send data to the BLE, the incident signal is received by different elements in SAA. It is assumed that incident signal consists of different packets, where each packet has a length of N_p samples, and N samples are received by one element before switching to the next element. After sending packet p_i through the data channel with the frequency f_j, the next packet p_{i+1} would be sent through $f_{j+1} = f_j + f_{hop}$. The wireless signal received at the BLE beacon, however, is the distorted version of the transmitted signal due to the deregulation of transmitter and receiver and the multipath and pathloss effects. Obtaining phase difference based on the raw data, therefore, leads to a noticeable error in angle estimation. For this reason, the first step towards angle detection is data processing, including phase compensation.

A. Noise Robustness

Owing to the existence of reflective obstacles, walls and movement of people, indoor environments suffer from multipath, shadowing, and pathloss effects. Therefore, BLEs receive a sum of different transmitted signal versions, where the interference of a large number of signals can cause either signal amplification or attenuation. For this reason, we eliminate this effect by applying Nonlinear Least Squares (NLS) curve fitting on the raw data. Given a function $f(t)$ of a variable t, a received packet p_i with N_p samples, including I/Q samples can be represented by

$$f_I(t; A_I, f_c, \phi_{I,0}) = A_I \sin(2\pi f_c t + \phi_{I,0}) \quad (7)$$

$$\text{and } f_Q(t; A_Q, f_c, \phi_{Q,0}) = A_Q \sin(2\pi f_c t + \phi_{Q,0}). \quad (8)$$

Our goal is to solve Eqs. (7) and (8) to obtain the best value of $\gamma_I \equiv (A_I, f_c, \phi_{I,0})$ and $\gamma_Q \equiv (A_Q, f_c, \phi_{Q,0})$ to diminish the effect of noise on the received signal. Toward this goal, first we pick an initial guess for γ_I and γ_Q, and define

$$d\beta_I \triangleq r_I(t) - f_I(t; A_I, f_c, \phi_{I,0}), \quad (9)$$

$$\text{and } d\beta_Q \triangleq r_Q(t) - f_Q(t; A_Q, f_c, \phi_{Q,0}). \quad (10)$$

To obtain a linearized estimate for the changes of γ_I and γ_Q, it is essential to achieve $d\beta_I = 0$ and $d\beta_Q = 0$. In this regard, we have $d\boldsymbol{\beta} = \mathbf{A}d\boldsymbol{\gamma}$, where $\mathbf{A}$ denotes a (2×3) matrix is defined as

$$\mathbf{A} = \begin{bmatrix} \frac{\partial f_I}{\partial A_I}|_{\gamma_I} & \frac{\partial f_I}{\partial f_c}|_{\gamma_I} & \frac{\partial f_I}{\partial \phi_{I,0}}|_{\gamma_I} \\ \frac{\partial f_Q}{\partial A_Q}|_{\gamma_Q} & \frac{\partial f_Q}{\partial f_c}|_{\gamma_Q} & \frac{\partial f_Q}{\partial \phi_{Q,0}}|_{\gamma_Q} \end{bmatrix}. \quad (11)$$

By applying the transpose of $\mathbf{A}$ to both sides, we have

$$\mathbf{A}^T d\boldsymbol{\beta} = (\mathbf{A}^T \mathbf{A}) d\boldsymbol{\gamma}. \quad (12)$$

Eq. (12) can be solved by applying standard matrix techniques such as Gaussian elimination. The best value of $\boldsymbol{\gamma}$ is obtained by using this method iteratively until $d\boldsymbol{\gamma}$ is smaller than a pre-defined threshold.

B. Eliminating Switching Error

As mentioned previously, we calculate the angle of incident signal based on the phase difference obtained from different elements. However, due to the phase shift of oscillator in both transmitter and receiver sides and also switching of elements, the value of $\boldsymbol{\Delta\Phi}^{(i,j)}$ for different i, j is not the same, leading to different values of $\boldsymbol{\theta}^{(i,j)}$. To solve this problem, we apply Kalman Filter (KF) on the phase difference obtained in different snapshots. To formulate the KF, an intermediate state vector $\boldsymbol{\Delta\hat{\Phi}}^{(i,j)}$ is defined, modeling the smoothed phase difference as the state-model given by

$$\boldsymbol{\Delta\hat{\Phi}}^{(i,j)}(k) = \boldsymbol{\Delta\hat{\Phi}}^{(i,j)}(k-1) + \boldsymbol{\rho}(k). \quad (13)$$

On the other hand, the observation model is defined by $\boldsymbol{\Delta\Phi}^{(i,j)} = \boldsymbol{\Delta\hat{\Phi}}^{(i,j)}(k) + \boldsymbol{\tau}(k)$, where the measured phase difference $\boldsymbol{\Delta\Phi}^{(i,j)}$ is used as the input observation to the KF. Terms $\boldsymbol{\rho}(k)$ and $\boldsymbol{\tau}(k)$ are Gaussian zero-mean variables used in the smoothing model with their second-order statistics ($\boldsymbol{Q}$ and $\boldsymbol{R}$) being obtained through an initial calibration phase.

C. Elimination of Frequency Error

There are 37 BLE channels to transmit data packets. However, it is evident that the angle obtained from different channels are different. One of the most important reason for that would be the interference of WiFi channels with BLEs. Therefore, it is essential to consider the impact of BLE's channel on the accurate angle. Toward this goal, after the calculation of phase difference based on Eq. (13), and calculating $\boldsymbol{\theta}^{(i,j)}$ in Eq. (6), the compensation vector $\boldsymbol{\chi}$ is defined to add to the estimated $\boldsymbol{\theta}^{(i,j)}$ to compensate the impact of BLE's channel. In this regard, we divide $-90^\circ \leq \theta \leq 90^\circ$ into 36 intervals, where $\theta_k = 5k - 90^\circ$, $k \in \{0, \ldots, 36\}$. For

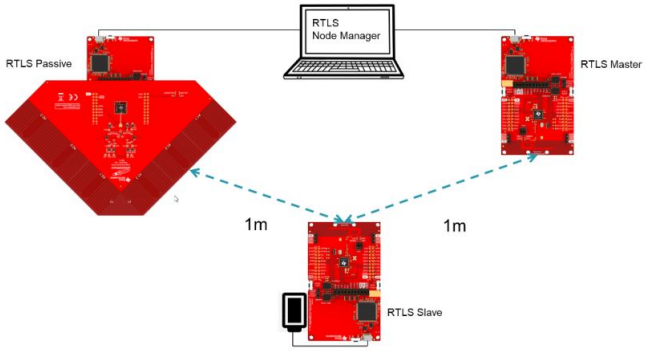

Fig. 3. The structure of RTLS Device, including RTLS Passive, Slave, and Master devices.

$-90^\circ \leq \theta \leq 90^\circ$ we obtain $\theta^{estimate}$ in all 37 channels in l iterations, and calculate the Mean Square Error (MSE) as

$$\omega_{k,ch} = \frac{1}{l} \sum_{q=1}^{l} (\theta_k - \theta_{ch,q}^{estimate})^2, \quad (14)$$

where $ch = 0, \ldots, 36$, and $k = 0, \ldots, 36$. In this case, we have a $(N_a \times N_{ch})$ coefficient matrix, denoted by $\boldsymbol{\omega}$, where N_a and N_{ch} denote the number of tested angles and the number of data channels in BLE technology, respectively. In this case, l^{th} column of matrix $\boldsymbol{\omega}$ denotes the MSE of angle θ_k in different channels. To obtain χ_{ch} associated with the compensation vector $\boldsymbol{\chi}$, we apply a Gaussian Filter (GF), denoted by $\mathcal{N}(\mu_{ch}, \sigma_{ch})$ on l^{th} column of matrix $\boldsymbol{\omega}$. Then, we obtain the final phase difference θ_{ch}^{final} as follows

$$\theta_{ch}^{final} = \theta_{ch}^{estimate} + \chi_{ch}. \quad (15)$$

IV. Experimental Results

The proposed wireless signal processing methods are applied on a real dataset consisting of I/Q samples collected by *SimpleLink Angle of Arrival Booster Pack*. As shown in Fig. 3, this package includes RTLS master, RTLS slave, and RTLS Passive consisting of two linear antenna arrays with three elements. Due to availability of two linear antenna arrays, RTLS Passive can support an area with $-180^\circ \leq \theta \leq 180^\circ$. Without loss of generality, we analyze the data obtained from one antenna array to support an area within $-90^\circ \leq \theta \leq 90^\circ$. Fig. 4 illustrates all data, we have from a transmission signal. The carrier frequency and space distance between each elements d_0 are 2.4 GHz and 3.5 cm, respectively. The sample frequency is 250 kHz. At the beginning of the connection, the RTLS master shares some connection parameters with the computer. The RTLS slave is a device that we want to find its location, and RTLS passive receives packets from the slave device in terms of I/Q samples. Each data packet consists of 511 I/Q samples, where each $N = 16$ samples received by one element, before switching to another one. We eliminate the last 31 samples in each packet, since there is no switching in transmission of these samples. It is assumed that the first packet is sent randomly on one of the BLE's channel, however, other packets are sent on the channels, selected based on

	A	B	C	D	E	F	G
1	pkt	sample_id	rssi	ant_array	channel	i	q
2	0	0	-56	1	28	-27	-112
3	0	1	-56	1	28	16	-113
4	0	2	-56	1	28	56	-101
5	0	3	-56	1	28	91	-75
6	0	4	-56	1	28	110	-42
7	0	5	-56	1	28	116	2
8	0	6	-56	1	28	105	43
9	0	7	-56	1	28	78	85
10	0	8	-56	1	28	43	111

Fig. 4. The raw received data sent from slave nodes received by SAA in passive RTLS.

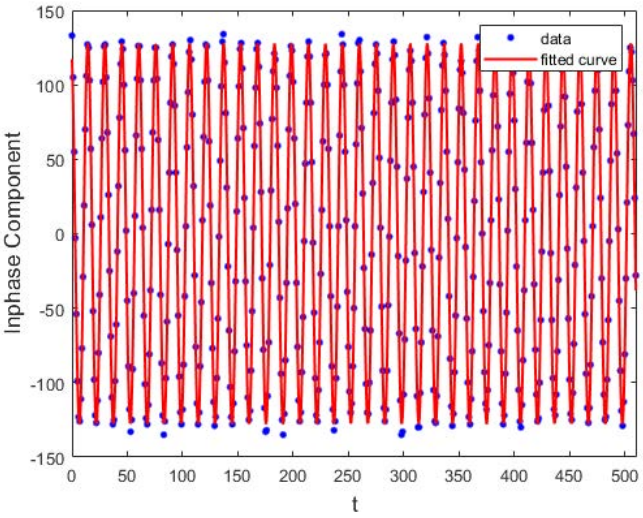

Fig. 5. Curve fitting for Inphase samples of a packet with the length of 511.

the FH method with $f_{hop} = 6$. After transmitting a packet completely, i.e., $N = 511$ samples, the received I/Q samples are fitted to sinusoidal signals based on the NLS curve fitting to eliminate the effect of noise on the data. Fig. 5 illustrates the real Inphase data and curve fitted signal.

To obtain the angle of arrival, we need to calculate the phase difference between signals received by different elements. In our case of study, the number of elements in an array antenna in the SAA is equal to 3. Therefore, we have 3 phase differences in each snapshot, including $\mathbf{\Delta\Phi}^{(1,2)}$, $\mathbf{\Delta\Phi}^{(2,3)}$, and $\mathbf{\Delta\Phi}^{(1,3)}$, where $\mathbf{\Delta\Phi}^{(1,2)} = \mathbf{\Delta\Phi}^{(2,3)} = \frac{1}{2}\mathbf{\Delta\Phi}^{(1,3)}$, since $d_{1,3} = 2d_{1,2} = 2d_{2,3}$.

As it can be seen from Fig. 6, there are specific phase differences between signals received by different elements. However, the value of phase difference is not equal for all samples in a particular packet. In addition, the value of $\mathbf{\Delta\Phi}^{(i,j)}$ for different i, j is not the same, leading to a remarkable error in the angle detection. This problem is tackled in our work by applying the KF on the phase difference obtained from different elements. To illustrate the performance of our processing method, we select 3 snapshots among $m = 10$ snapshots collected during one packet, including the first, the middle and the last one, to investigate the phase difference

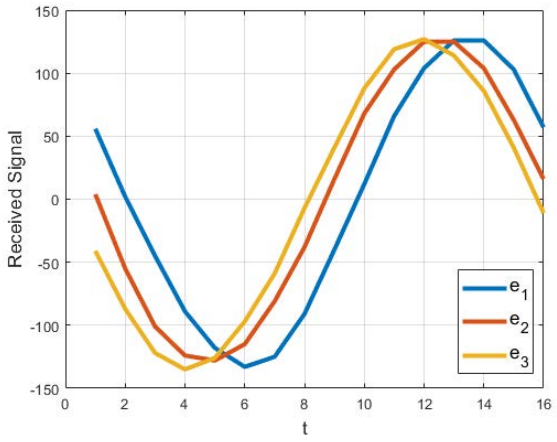

Fig. 6. Phase difference between signals received by different elements in SAA.

between different elements. According to the results shown in Tables I and II, by applying NLS curve fitting and KF on raw data, the phase difference obtained from different samples and different elements are the same, resulting in a low error in angle detection.

TABLE I
PHASE DIFFERENCES OBTAINED FROM DIFFERENT ELEMENTS BEFORE APPLYING KF, WHERE $\theta_{real} = -4$ DEGREE, AND THE REAL VALUE OF PHASE DIFFERENCES SHOULD BE EQUAL TO $\mathbf{\Delta\Phi}^{(1,2)} = -8$, $\mathbf{\Delta\Phi}^{(2,3)} = -8$, AND $\mathbf{\Delta\Phi}^{(1,3)} = -16$ DEGREE.

Type	1st snapshot	5th snapshot	10th snapshot
$\mathbf{\Delta\Phi}^{(1,2)}$	-3.9423	-15.3012	-10.2659
$\mathbf{\Delta\Phi}^{(2,3)}$	-11.3190	-12.9405	3.5454
$\mathbf{\Delta\Phi}^{(1,3)}$	-15.2613	-28.2418	-6.7205

TABLE II
PHASE DIFFERENCES OBTAINED FROM DIFFERENT ELEMENTS AFTER APPLYING KF, WHERE $\theta_{real} = -4$ DEGREE, AND THE REAL VALUE OF PHASE DIFFERENCES SHOULD BE EQUAL TO $\mathbf{\Delta\Phi}^{(1,2)} = -8$, $\mathbf{\Delta\Phi}^{(2,3)} = -8$, AND $\mathbf{\Delta\Phi}^{(1,3)} = -16$ DEGREE.

Type	1st snapshot	5th snapshot	10th snapshot
$\mathbf{\Delta\Phi}^{(1,2)}$	-8.1851	-8.1813	-8.2438
$\mathbf{\Delta\Phi}^{(2,3)}$	-8.1704	-8.1824	-8.2539
$\mathbf{\Delta\Phi}^{(1,3)}$	-16.3555	-16.3909	-16.5578

Considering the fact that there are 37 data channels for transmitting signal, each packet is being sent on different frequency, in which $f_c = 2.4 \times 10^9 + (\kappa + 2) \times 2 \times 10^6$ for $(0 \leq \kappa \leq 10)$, and $f_c = 2.4 \times 10^9 + (2\kappa + 3) \times 10^6$ for $(11 \leq \kappa \leq 36)$. Due to the same frequency bandwidth between WiFi and BLE technologies, BLE technology suffers from interference with WiFi. As a result, the value of θ needs to be compensated after the AoA is measured due to variability in results through frequency. Therefore, a constant offset $\boldsymbol{\chi}$, which is calculated based on the GF is applied on different frequencies to boost performance of the BLE-based AoA estimation. Table III shows the compensation values used for each frequency.

TABLE III
FREQUENCY COMPENSATION χ OVER ALL BLE CHANNELS.

Channel	37	0	1	2	3
χ_{ch}	0	-2	-4	7	15
Channel	4	5	6	7	8
χ_{ch}	18	14	8	6	5
Channel	9	10	38	11	12
χ_{ch}	1	1	0	3	5
Channel	13	14	15	16	17
χ_{ch}	8	9	10	13	11
Channel	18	19	20	21	22
χ_{ch}	-5	-3	-2	1	0
Channel	23	24	25	26	27
χ_{ch}	3	5	8	12	15
Channel	28	29	30	31	32
χ_{ch}	15	-7	5	8	4
Channel	33	34	35	36	39
χ_{ch}	2	3	1	-4	0

Fig. 7 compares the angle estimation error of our proposed processing method with such a case where there is no processing techniques on raw data. Accordingly, our proposed framework significantly reduces the AoA error and displays errors of less than 10° on most frequencies from -60° to 60°. It is worth mentioning that when the signal propagation direction is near parallel to the antenna array, the phase difference are almost random. Therefore, there exists a considerable error from -60° to -90° and 60° to 90° for most frequencies, due to the hardware setup of our device.

V. CONCLUSION

In this paper, we proposed an efficient processing framework to estimate the BLE-based angle of incident signal through the phase difference between I/Q samples received by different element embedded on a SAA. To decrease the sensitivity of AoA localization to multipath effects, NLOS, fluctuations of received signal, and frequency and phase shiftings, we employed Nonlinear Least Square (NLS) curve fitting, Kalman Filter (KF), and Gaussian Filter (GF) on raw I/Q samples. The presented methodology was validated on a real BLE dataset collected by *SimpleLink Angle of Arrival Booster Pack*. Our simulation results shown that the proposed processing framework can achieve accurate angle estimation.

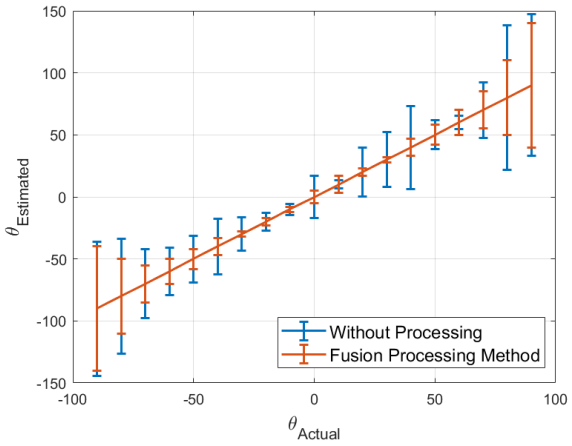

Fig. 7. Compensated AoA after applying NLS curve fitting, KF, and GF.

REFERENCES

[1] M. Ozcan, A. Fuad, and G. Haluk, "Accurate and Precise Distance Estimation for Noisy IR Sensor Readings Contaminated by Outliers," Elsevier: Measurement, vol. 156, pp. 1–13, Feb. 2020.

[2] R. Carotenuto, M. Merenda, D. Iero, and F. G. D. Corte, "Mobile Synchronization Recovery for Ultrasonic Indoor Positioning," Sensors, vol. 20, no. 3, pp. 702–727, Jan. 2020.

[3] M. Maheepala, A. Z. Kouzani, and M. A. Joordens, "Light-based Indoor Positioning Systems: A Review," IEEE Sensors Journal, Jan. 2020.

[4] G. W. Samu, and P. Kadam, "Survey on Indoor Localization: Evaluation Performance of Bluetooth Low energy and Fingerprinting based Indoor Localization System," International Journal of Computer Engineering and Technology (IJCET), vol. 8, no. 6, pp. 23–35, Dec. 2017.

[5] A. Loganathan, N. S. Ahmad, and P. Goh, "Self-Adaptive Filtering Approach for Improved Indoor Localization of a Mobile Node with Zigbee-Based RSSI and Odometry," Sensors, vol. 19, no. 21, pp. 4748–4773, Jan. 2019.

[6] S. Weiguang, J. Du, X. Cao, Y. Yu, Y. Cao, S. Yan, and C. Ni, "IKULDAS: An Improved kNN-Based UHF RFID Indoor Localization Algorithm for Directional Radiation Scenario," Sensors, vol. 19, no. 4, pp. 968–986, Jan. 2019.

[7] G. Huang, Z. Hu, J. Wu, H. Xiao, and F. Zhang, "WiFi and Vision Integrated Fingerprint for Smartphone-Based Self-Localization in Public Indoor Scenes," IEEE Internet of Things Journal, Feb. 2020.

[8] P. Malekzadeh, A. Mohammadi, M. Barbulescu, and K. N. Plataniotis, "STUPEFY: Set-Valued Box Particle Filtering for Bluetooth Low Energy-Based Indoor Localization," IEEE Signal Processing Letters, vol. 26, no. 12, pp. 1773–1777, Dec. 2019.

[9] J. J. P. Solano, S. Ezpeleta, and J. M. Claver, "Indoor localization using time difference of arrival with UWB signals and unsynchronized devices," Elsevier: Ad Hoc Networks, vol. 99, pp. 1–11, Mar. 2020.

[10] M. Atashi, M. Salimibeni, P. Malekzadeh, M. Barbulescu, K. N. Plataniotis, and A. Mohammadi, "Multiple model BLE-based tracking via validation of RSSI fluctuations under different conditions," International Conference on Information Fusion (FUSION), July 2019, pp. 1–6.

[11] S. Mehryar, P. Malekzadeh, S. Mazuelas, P. Spachos, K. N. Plataniotis, and A. Mohammadi, "Belief condensation filtering for RSSI-based state estimation in indoor localization," IEEE International Conference on Acoustics, Speech and Signal Processing (ICASSP), May 2019, pp. 8385–8389.

[12] S. Monfared, T. Nguyen, L. Petrillo, P. De Doncker, and F. Horlin, "Experimental Demonstration of BLE Transmitter Positioning Based on AOA Estimation," IEEE International Symposium on Personal, Indoor and Mobile Radio Communications (PIMRC), Bologna, Dec. 2018, pp. 856-859.

[13] P. Spachos, I. Papapanagiotou and K. N. Plataniotis, "Microlocation for Smart Buildings in the Era of the Internet of Things: A Survey of Technologies, Techniques, and Approaches," IEEE Signal Processing Magazine, vol. 35, no. 5, pp. 140–152, Sep. 2018.

[14] N. H. Nguyen, and K. Dogancay, "Closed-Form Algebraic Solutions for Angle-of-Arrival Source Localization With Bayesian Priors," IEEE Transactions on Wireless Communications, vol. 18, no. 8, May 2019, pp. 3827–3842.

[15] M. Kulin, T. Kazaz, I. Moerman, and E. De Poorter, "End-to-End Learning From Spectrum Data: A Deep Learning Approach for Wireless Signal Identification in Spectrum Monitoring Applications," IEEE Access, vol. 6, pp. 18484-18501, March 2018.

[16] M. Cominelli, P Patras, and F Gringoli. "Dead on Arrival: An Empirical Study of The Bluetooth 5.1 Positioning System," International Workshop on Wireless Network Test beds, Experimental Evaluation and Characterization, pp. 13-20. Oct. 2019.

[17] Y. Lin, T. Guo, M. Guo, and Y. Fu, "Motion Compensation for SAA FMCW Radar Based on Specific Switching Scheme," Applied Sciences, vol. 9, no. 17, pp. 3441–3449, Jan. 2019.

[18] A. Nikoukar, M. Abboud, B. Samadi, M. Guneş, and B. Dezfouli, "Empirical analysis and modeling of Bluetooth Low-Energy (BLE) advertisement channels," Mediterranean Ad Hoc Networking Workshop, Capri, July 2018, pp. 1-6.